# HARPS-N @ TNG, two years harvesting data: Performances and results

Rosario Cosentino[1], Christophe Lovis[2,] Francesco Pepe[2], Andrew Collier Cameron[3], David W. Latham[4], Emilio Molinari[1], Stephane Udry[2], Naidu Bezawada[6], Nicolas Buchschacher[2], Pedro Figueira[5], Michel Fleury[2], Adriano Ghedina[1], Alexander G. Glenday[4],Manuel Gonzalez[1], Jose Guerra[1], David Henry[6], Ian Hughes[2], Charles Maire[2], Fatemeh Motalebi[2], David Forrest Phillips[4]

1-INAF – TNG, 2-Observatoire Astronomique de l'Université de Genève Switzerland, 3-SUPA, School of Physics & Astronomy University of St Andrews UK, 4-Harvard-Smithsonian Center for Astrophysics USA, 5- Centre for Star and Planet Formation, Natural History Museum of Denmark, 6-UK Astronomy Technology Centre, Royal Observatory, Blackford hill, Edinburgh, UK

## ABSTRACT

The planet hunter HARPS-N[1], in operation at the Telescopio Nazionale Galileo (TNG)[13] from April 2012 is a high-resolution spectrograph designed to achieve a very high radial velocity precision measurement thanks to an ultra stable environment and in a temperature-controlled vacuum. The main part of the observing time was devoted to Kepler field and achieved a very important result with the discovery of a terrestrial exoplanet. After two year of operation, we are able to show the performances and the results of the instrument.

**Keywords:** Telescopio Nazionale Galileo, HARPS-North, high resolution, spectrograph, instrumentation, telescope, exoplanets, radial velocity

## 1. INTRODUCTION

The planet hunter HARPS-N began its commissioning phase at the Telescopio Nazionale Galileo (TNG) in April 2012 and in August was offered to the astronomical community. HARPS-N is an echelle spectrograph which allows the measurement of radial velocities with the highest accuracy available in the northern hemisphere and is designed to avoid spectral drifts due to temperature and air pressure variations via very accurate control of these parameters.
HARPS-N dedicated a large amount of observation time to the follow-up of candidates identified by the Kepler satellite and to search for rocky planets in the habitable zones of solar-like stars in the GTO project and is also involved in the long term Italian national program GAPS to investigate various aspect of astronomy that require high precision and stability.
In these two years of operation we spent our efforts to maintain and increase the performances of the instrument that works as expected and collects very remarkable results.

## 2. GENERAL CHARACTERISTICS

HARPS-N is a fiber-fed, cross-dispersed echelle spectrograph, based on the design of its predecessor working at ESO 3.6 m[14]. This successful spectrograph already has proven its capability to achieve a precision better than 1 meter per second and revealed several super-earth planets in the habitable zone.
Two fibers, an object and a reference fiber of 1 arcsec aperture pick up the light at the Nasmyth B focus of the telescope and feed the spectrograph either with calibration or stellar light. The fiber entrance is re-imaged by the spectrograph optics onto a 4k×4k CCD, where echelle spectra of 69 orders are formed for each fiber. The covered spectral domain ranges from 390 nm to 690 nm. The resolution of the spectrograph is given by the fiber diameter and reaches an average value of R = 115000. The spectrograph is mounted on a nickel-plated stainless steel mount and contains no moving parts. Furthermore, in order to avoid spectral drifts due to temperature and air pressure variations, it is accurately controlled in pressure and temperature. In Figure 1 the mechanical mount (on the left) and the installation inside the vacuum vessel (on the right) are shown. A summary of the main HARPS characteristics is given in Table 1.

**Figure 1 – HARPS-N mechanical design and vacuum vessel**


**Table 1 – HARPS-N main characteristics**

| | |
|---|---|
| Spectrograph type | Fiber fed, cross-dispersed echelle spectrograph |
| Spectral resolution | R = 115'000 |
| Fiber field | FOV = 1" |
| Wavelength range | 383 nm - 690 nm |
| Total efficiency | e = 8 % @ 550 nm (incl. telescope and atmosphere @ 0.8" seeing) |
| Sampling | s = 3.3 px per FWHM |
| Calibration | ThAr + Simultaneous reference  (fed by 2 fibers) |
| CCD | Back-illuminated 4k4 E2V  CCD231 (graded coating) |
| Pixel size | 15 μm |
| Environment | Vacuum operation -   0.001 K temperature stability |
| Global short-term precision | 0.3 m/s |
| Global long-term precision | Better than 0.6 m/s |
| Observational efficiency | SNR = 50 per extracted pixel on a Mv=8, TExp = 60 sec |
| wavelength accuracy | 60 m/s (2x10E-7) on a single line |


## 3. THE DATA REDUCTION SOFTWARE (DRS)

The Data reduction Software (DRS)[15], developed at the same time of the instrument, was modified along the operation period. Some procedures were fine-tuned and others were added in order to improve the precision and more features to the astronomer. All the realized improvements led to a high efficiency instrument for the TNG Observatory[12].

### 3.1 CTE correction

Raw frames are corrected for charge transfer inefficiency by estimating the amount of charge that was left behind in each pixel along CCD columns. The "lost" charge is added back to the original pixel it belongs to, and subtracted from the pixel it ended in. The Charge Efficiency Transfer (CTE) is a flux-dependent effect that is proportionally larger at low fluxes, inducing systematic offsets in radial velocities as a function of SNR. CTE correction was calibrated on test data taken at different signal levels, and then validated on both calibration and science data.

### 3.2 Color correction

Broadband fluctuations in the measured spectral energy distribution of target stars due to variable seeing and weather conditions induce subtle effects on derived cross-correlation functions (CCFs) and radial velocities at the m/s level. To correct for this effect, target spectra are first normalized in flux based on template spectra obtained with HARPS-N for

various spectral types. The correction not only improves radial velocity precision, but also stabilizes other CCF parameters such as FWHM and bisector span. This makes it possible to use these parameters for stellar activity monitoring.

## 3.3 Background/crosstalk reduction

The optimal extraction algorithm used by the pipeline has been further improved to include the modeling and removal of contamination light from the simultaneous reference spectrum (ThAr or Fabry-Perot). The extraction profile in cross-dispersion direction is modelled as a linear combination of the empirical order profile obtained from spectral flat-field exposures and the empirical "contamination profile" from fiber B obtained from ThAr-only or FP-only exposures. In this way the extracted science spectrum can be cleaned from the direct crosstalk induced by saturated emission lines on fiber B.

## 3.4 RHK calculation

The computation of the Ca II H & K activity index log(R'HK) has been implemented in the pipeline. The algorithm first computes the Mt Wilson S-index from the measured fluxes in the Ca II line cores and two adjacent continuum regions. The S-index is then converted to log(R'HK) using calibration provided in the literature based on the B-V color of the target star. HARPS-N delivers high-precision measurements of the Ca II activity index, which allow the user to monitor the stellar magnetic activity level even for chromospherically quiet stars.

## 4. HARPS-N STABILITY

### 4.1 The simultaneous reference technique

To reach such precise measurement of radial velocity, the spectrograph removes possible residual instrumental drifts from the measured RV and guarantees an accurate localization of the wavelength in the detector with the simultaneous reference technique. For this purpose HARPS-N uses two fibers, which feed the spectrograph simultaneously and forms two well-separated spectra on the CCD detector. Both fibers are wavelength calibrated at the beginning of the night. During scientific observations the first fiber is fed with the star light, and on this spectrum the stellar radial velocity is computed by referring to the wavelength solution determined at the beginning of the night. The second fiber is illuminated with the same spectral reference all the time, during wavelength calibration and scientific exposures. If an instrumental drift had occurred in between, the simultaneous reference spectrum on the second fiber would measure it.

In the following chapters we will show the short-term drift and a long-term statistic of the drift, measured for the ThAr lamp and for the Fabry-Perot calibrator.

### 4.2 The instrumental stability and the ThAr simultaneous reference

To demonstrate the extraordinary short-term stability of the HARPS-N spectrograph we monitored the instrumentally induced velocity change (drift) by measuring the position of the ThAr emission lines on the two fibers along 18 consecutive hours.

The series of measurements in Figure 2 shows that the radial velocity remains stable within the 1 m/s level.

The drift-corrected radial velocity ( RVb –RVa) shown in Figure 3 demonstrate that the simultaneous reference technique is able to correct for drift at the level below of 10 cm/s.

The big amount of calibration data collected during the last two years of HARPS-N operation can be used to estimate the drift-corrected standard velocity behavior. In the Figure 4 is shown the distribution of RVb-RVa in the period from the beginning of 2013 to mid-May.

The photons noise of the Radial Velocity measured on the fibers, in the ThAr calibration, is 0.046 m/s for the fiber A and 0.056 m/s for the fiber B. This means that the internal error in single drift measurements is about 0.07 m/s (0.065 for the fiber A and 0.072 for the fiber B) and the internal error in the RVb –RVa measurement is on the order of 0.1 m/s.

The drift-corrected radial velocity distribution calculated with more than 1600 ThAr calibration spectra shows a standard deviation of 0.138 m/s. The difference between the calculated distribution and the internal error predicted is due to a combination of the long term drift of 10 cm/s/day, due to a opto-mechanical effect and measured with the laser-comb (see figure 10 B) and a ThAr lamps effect due to the different emission of the ThAr A and ThAr B lamps.

The comparison between the experimental measurements along 22 months and the internal error is very satisfactory and demonstrates that the statistical noise is as expected, taking into account the effects mentioned above.
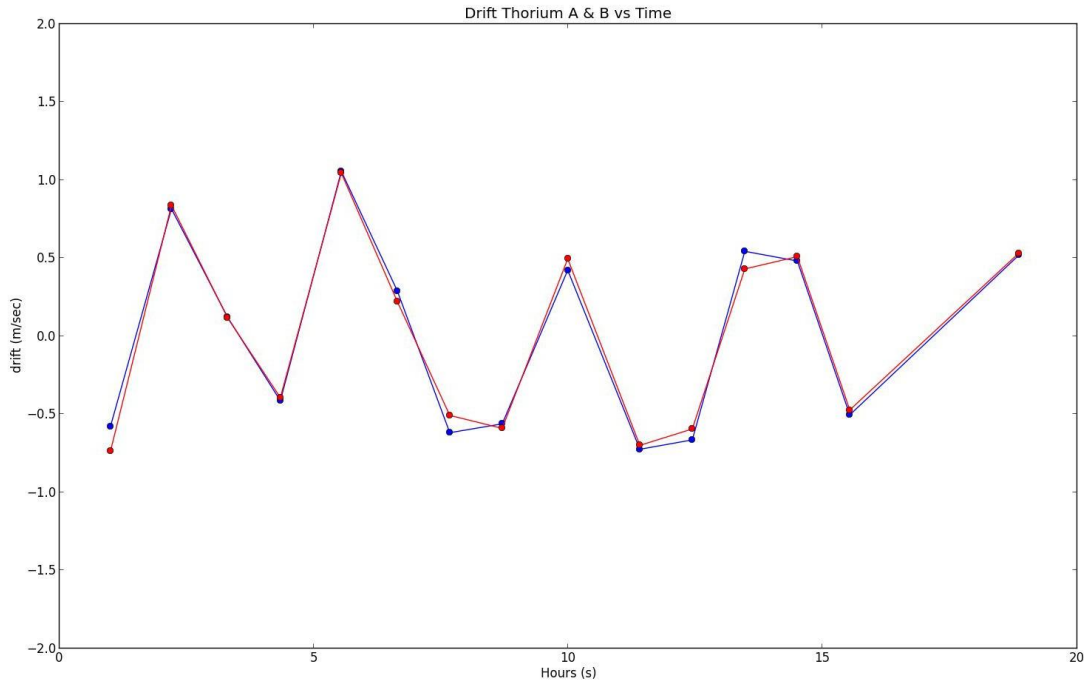
**Figure 2 - Series of radial-velocity measurements on ThAr calibration. The red and blue points represent the instrumentally induced velocity change during 18 consecutive hours on the fiber A and fiber B (RVa and RVb)**
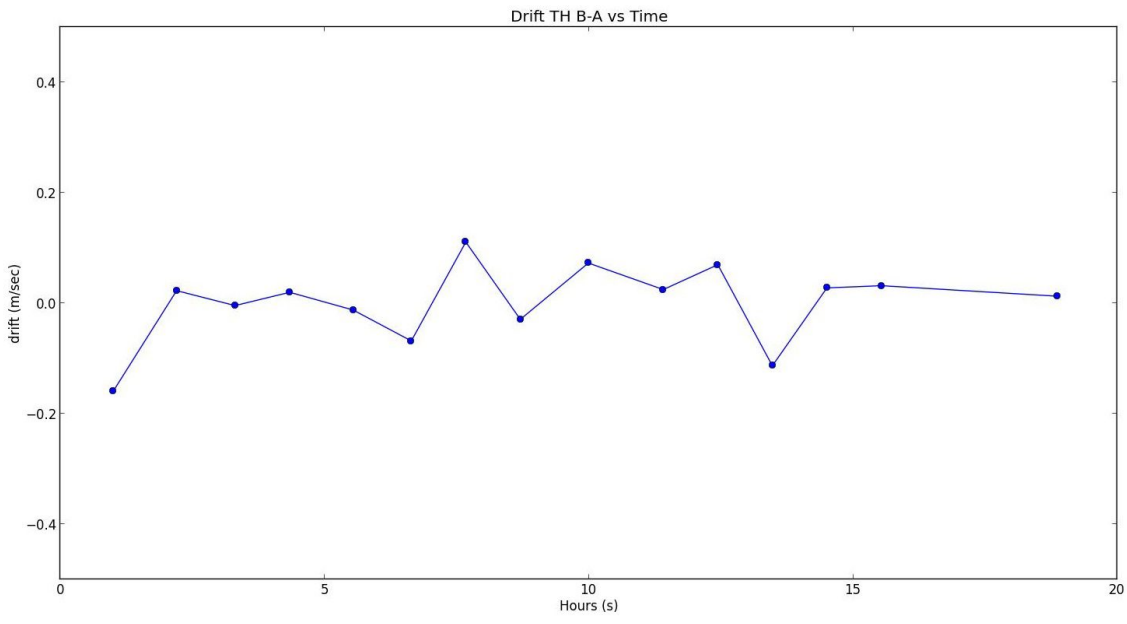
:



**Figure 3 - Plot of the difference between the RV drift measured by the A and B fiber of the series in Figure 3**
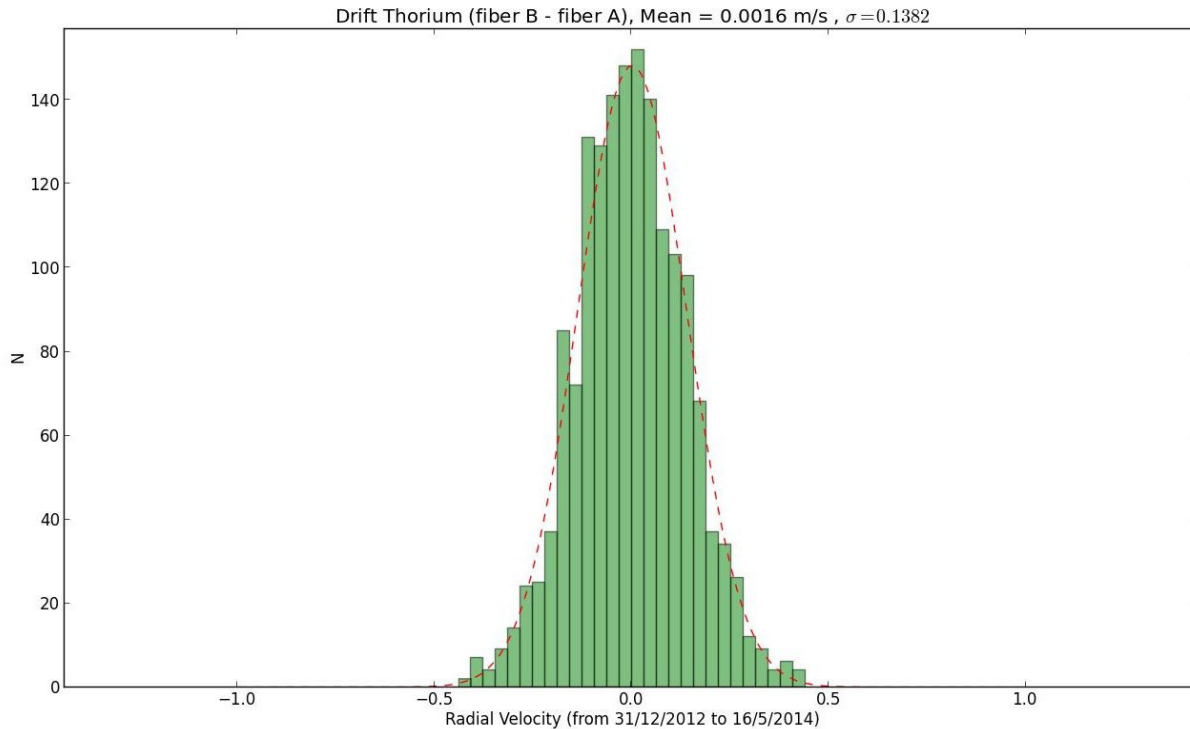
…

**Figure 4 – drift-corrected radial velocity distribution (RVb -RVa) calculated with more than 1600 ThAr calibration spectra, in in a time period of 22 months**

## 4.3 The Fabry-Perot simultaneous reference[17]

Likewise we monitored the instrumentally induced velocity change (drift) by measuring the position of the Fabry-Perot emission lines on the fiber B and the ThAr lamp on the fiber A along 18 consecutive hours.
The series of measurements in Figure 5 shows that the radial velocity remains stable within a little more than 1 m/s level.
The drift-corrected radial velocity (RVb –RVa) shown in Figure 6 demonstrate that the simultaneous reference technique is able to correct for drift at the level below of 30 cm/s. The FP also may drift at the level of 30 cm/s over 24 hours or 15 cm/s in a night. We are working to make it even more stable.

As in the ThAr case, we estimated the drift-corrected standard velocity behavior. We measured the distribution of RVb-RVa in the period from the beginning of 2013 to mid-May.
The photons noise of the Radial Velocity measured on the fibers, in the Fabry-Perot calibration, is 0.046 m/s for the fiber A and 0.024 m/s for the fiber B. This means that the internal error in single drift measurements is 0.065 for the fiber A and 0.051 for the fiber B and the internal error in the RVb –RVa measurement is on the order of 0.082 m/s.
The drift-corrected radial velocity distribution calculated with more than 1600 ThAr calibration spectra shows a standard deviation of 0.28 m/s.
The difference between the experimental measurements along 22 months and the internal error is higher than the expected. The cause can be the problem of stability of the Fabry-Perot at the beginning of the HARPS-N operations, fixed in the last intervention on HARPS-N and the contamination of the data sample with values taken during the laser-comb test. In the next months we will acquire a new set of data in a better operative condition to calculate a more reliable value.
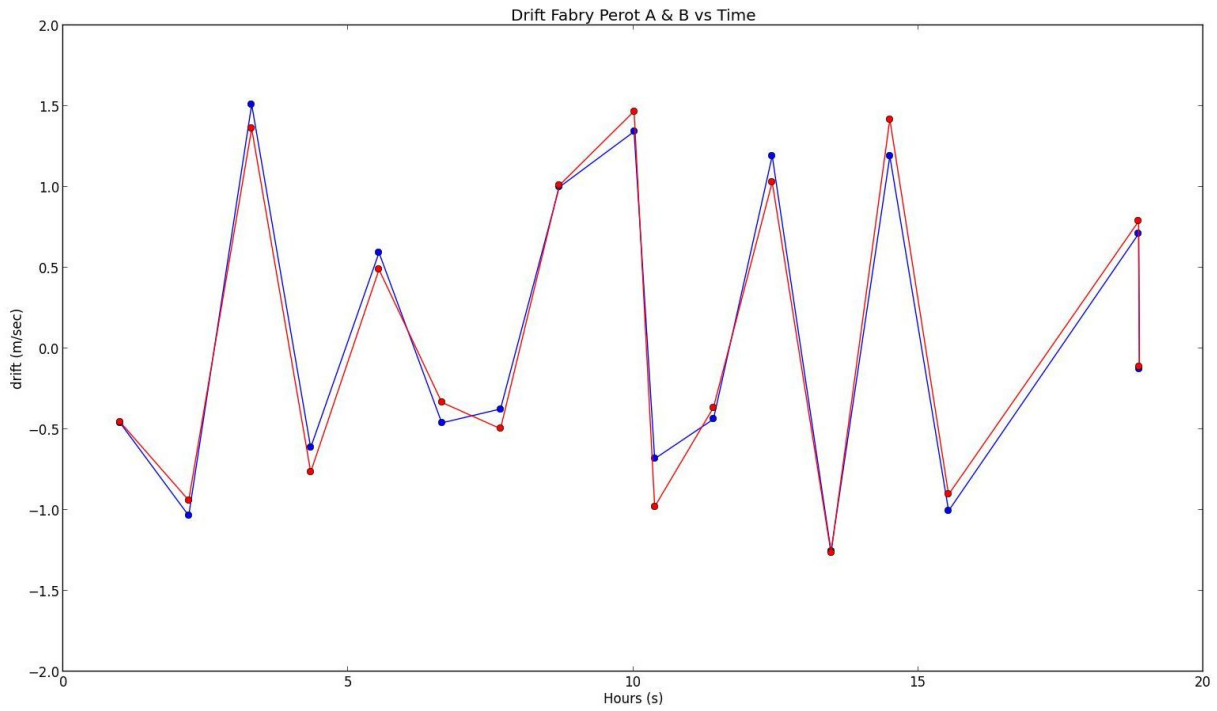
**Figure 5 -- Series of radial-velocity measurements on Fabry-Perot. The red and blue points represent the instrumentally induced velocity change during 18 consecutive hours on the fiber A and fiber B (RVa and RVb)**
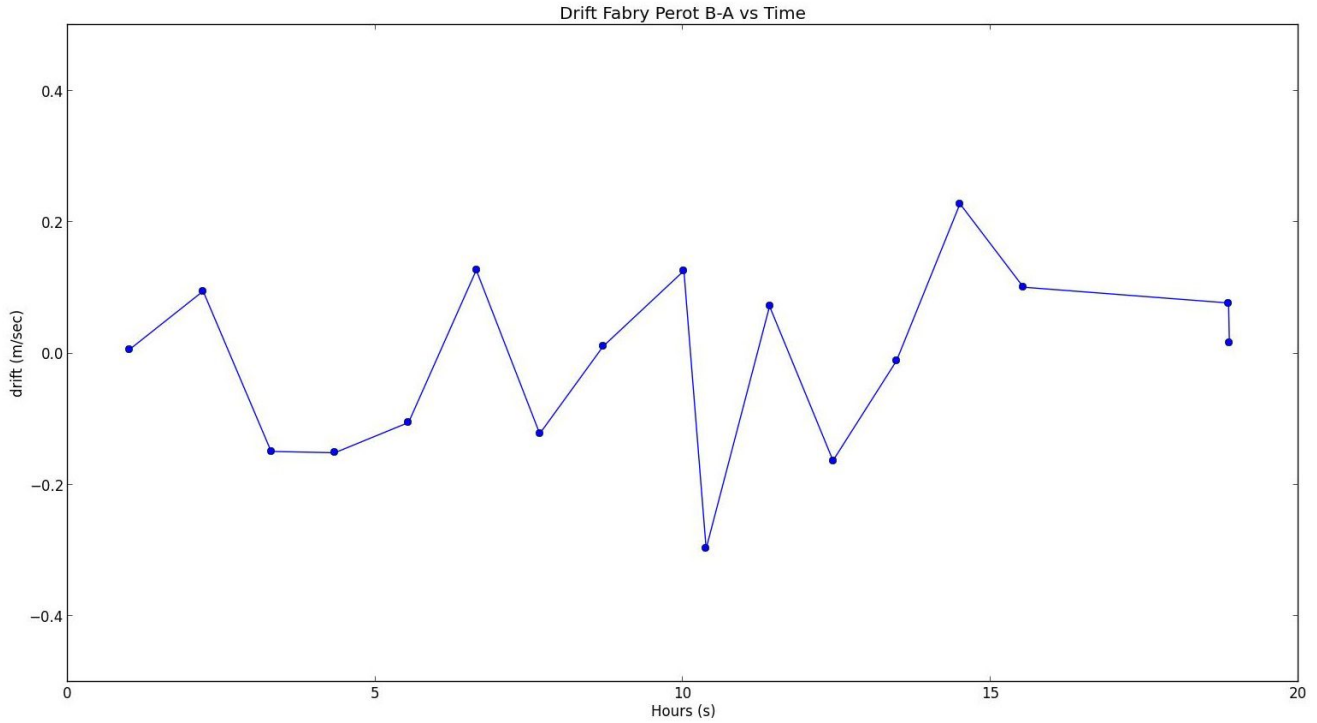


**Figure 6 - Plot of the difference between the RV drift measured by the A and B fiber of the series in Figure 5**

# 5. RADIAL VELOCITY PRECISION

## 5.1 Radial velocity dispersion measured on a RV standard star

The radial velocity precision obtained on a given star depends on many factors, not the least being the stellar intrinsic noise or jitter. Nevertheless, even for a 'quiet' star, the obtained precision depends on the spectral lines widths, depths, and densities, which all depend partially on the spectral type. In order to provide a statistic of measured radial-velocity precision, we focus on the quiet, non-rotating star HD166620, observed for 21 months, from June 2012 to March 2014 in the GTO long-term program.

In this case, the radial velocity dispersion over 21 months and 309 exposures is of 1.29 m/s, in agreement with the expected value. Figure 7 shows the temporal distribution of the measures of HD166620;
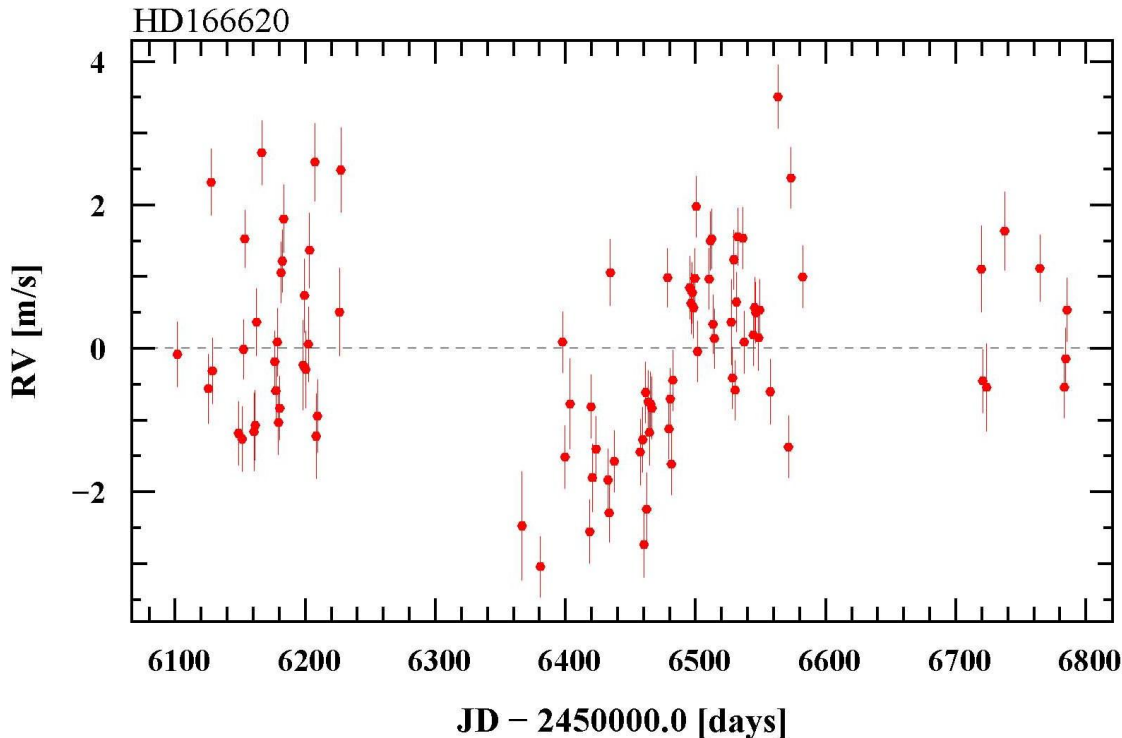


**Figure 7 - series of radial velocity measurements on HD166620**

## 5.2 Distribution of the RV dispersion in a sample of stars

In Figure 8 is shown the distribution of the radial velocity dispersion of the RPS sample contains 45 stars with at least three measurements over the last two years; most of the RPS star have a magnitude between 5 and 8 and the distribution of RV is centred on 2 m/s. If you consider that the rms contains the external noise due to photo noise, stellar noise, potential planetary signals, etc. and that it is only an upper limit for residual instrumental noise, the fact that the are target with rms below 2 m/s demonstrate the high precision of HARPS-N in the measurement of radial velocity.
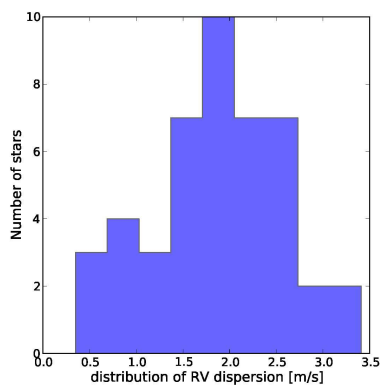
**Figure 8 – Distribution of RV dispersion on a RPS GTO sample**

## 5.3 Comparison of RV dispersion with other instruments

The RV of the planetary system HD 3651, which hosts a giant planet, was measured by various telescopes[18]. We have compared the RV dispersion of HARPS-N on TNG, with Hamilton on Lick and with HIRES on Keck.
This example clearly shows the increase in performance of HARPS-N at the TNG with respect to other available instruments.
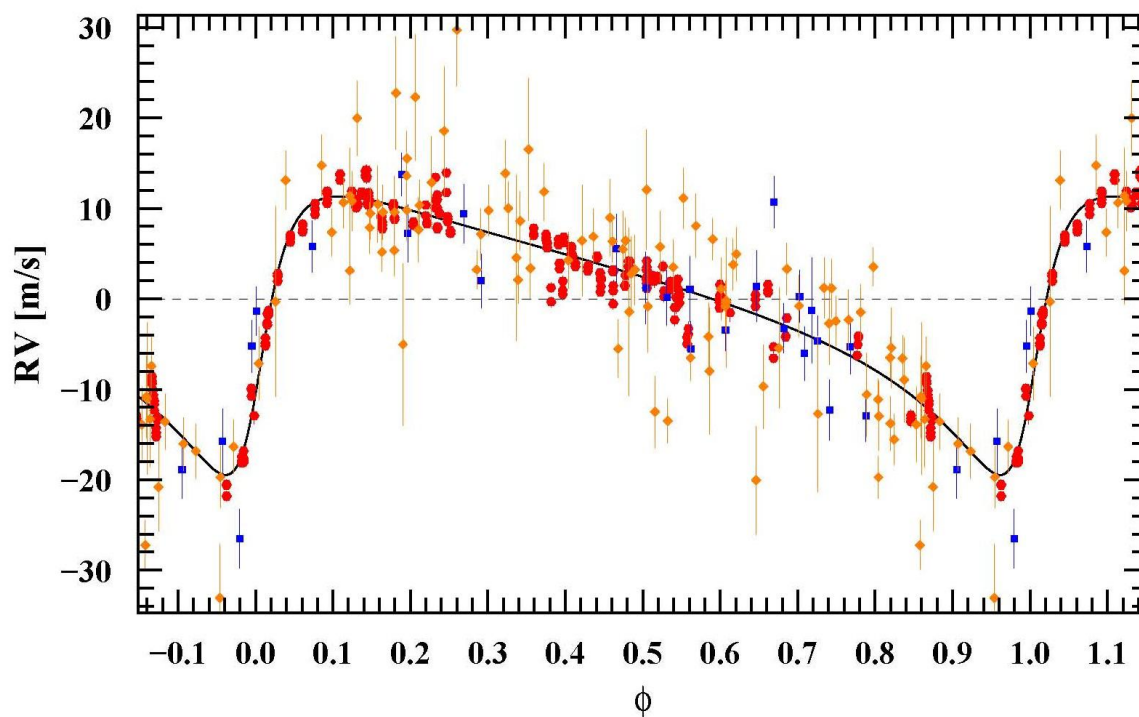The values of the dispersions for this tree instruments are shown in Figure 9 and are resumed in Table 2.



**Figure 9 - RV dispersion of HD3651 measured with different instruments; HARPS-N(red), Hamilton(orange),Hires(blue)**

**Table 2 RV dispersion**

| RV Dispersion | | |
|---|---|---|
| HARPS-N (TNG) | 1.82 m/s | Red points |
| Hamilton (Lick) | 5.86 m/s | Orange points |
| HIRES (Keck) | 3.88 m/s | Blue points |

## 6. THE ASTRO-COMB WAVELENGHT CALIBRATOR FOR HARPS-N

An astro-comb, a high precision wavelength calibrator, has been operating at the TNG-N for use with HARPS-N since January of 2013. Our astro-comb calibrates in the green-orange spectral range from 5000-6200 Å.

In a series of measurements, the astro-comb has been used to (i) calibrate the HARPS-N spectrograph, (ii) determine the instrument line profile in the spectral range over which calibration light is available, (iii) characterize the performance of the HARPS-N spectrograph, and (iv) monitor the differential drift between the calibration of the science and calibration fibers.

### 6.1 The laser-comb with HARPS-N

The astro-comb[7], as represented schematically in Fig. 1, consists of a high repetition rate, octave spanning, pulsed titanium-sapphire laser with the following characteristics: (a) a center wavelength of 8000 Å, (b) a 1 GHz pulse repetition rate; (c) roughly 6 femtosecond pulse lengths corresponding to a 1500 Å FWHM spectrum whose optical frequencies are stabilized to a GPS-referenced atomic clock providing better than $10^{-12}$ fractional accuracy. Each optical line is separated by 1 GHz (0.02 Å at 8000 Å). These lines are coherently shifted into the green/orange visible spectrum using a custom tapered photonic crystal fiber (PCF) and matched to the resolution of the HARPS-N spectrograph using a pair of Fabry-Perot filter cavities stabilized to the comb itself via a single wavelength reference laser. To avoid speckle (pattern) noise on the re-imaged comb spectrum on the spectrograph CCD, phase coherence is destroyed using a mechanical shaker[8]-[10].

The astro-comb produces approximately 7000 calibration lines with an intrinsic line width of < 1 MHz (under 0.001 of the resolution of HARPS-N). Figure 10(b) shows a small section of the astro-comb spectrum in one order.

The line profile is that of the spectrograph with a FWHM~ 3.5 pixels and a calibration uncertainty of roughly 2.5 m/s for one peak in a 10 second exposure. We achieve a typical peak SNR of > 350 for the astro-comb as measured by HARPS-N. Calibrating both the science and calibration fibers of HARPS-N, we typically realize a single exposure RV calibration of HARPS-N with a one-sigma uncertainty ~ 6 cm/s (Figure 11 (a)), which is within 10% of the theoretical SNR due to photon shot noise. Repeated measurements of the difference in wavelength calibration between the two fibers shows < 2 cm/s standard deviation after 16 exposures. After days to weeks of calibration, we observe a drift in calibration of roughly 10 cm/s/day (Figure 11 (b)).
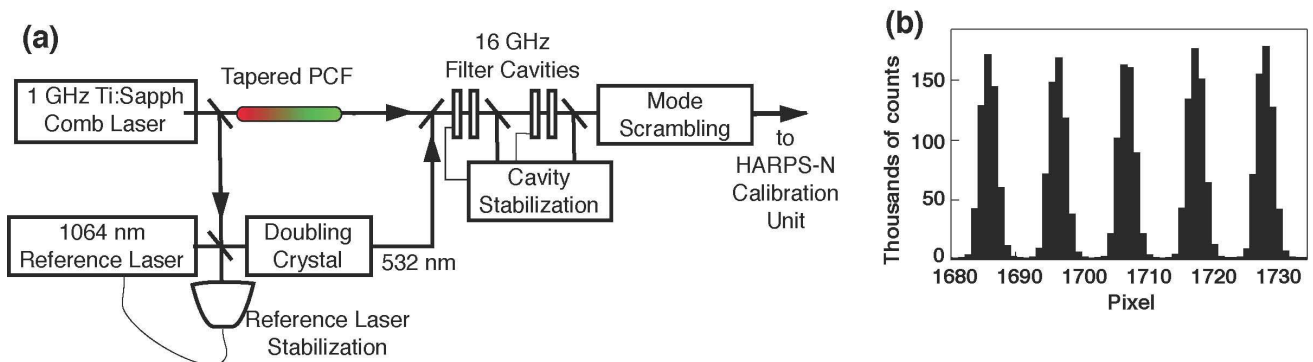
Figure 10 - Schematic of key components of astro-comb optics. Source comb lines spanning an octave in the near infrared with 1 GHz spacing are generated by an octave-spanning femtosecond titanium-sapphire laser, and stabilized to an atomic clock referenced to GPS for long term stability. A custom-tapered photonic crystal fiber (PCF) coherently shifts the comb lines to visible wavelengths. Two broadband Fabry-Perot cavities (FPCs) then filter the comb light, passing every 16th spectral line and suppressing all intermediate lines to increase the line spacing to 16 GHz (0.15 Å at 5300 Å). A cwNd:YAG laser (1.064 µm) is phase-locked to one of the source comb lines and frequency doubled in a periodically poled lithium niobate (PPLN) crystal to 5320 Å after which it is used to lock to the FPCs via a Pound-Drever-Hall type scheme. (b) Small portion of astro-comb spectrum from one order near 6000 Å.

The uniform comb feature spacing, high SNR, and delta function line profile of the astro-comb make it an ideal instrument for characterizing the performance of the HARPS-N spectrograph. We have performed a series of measurements monitoring the line profile of the HARPS-N instrument using the astro-comb and observe line shapes consistent with the design of HARPS-N. Additionally, we observe pixel size variation consistent with mask errors[11]. To extract mask errors, we fit each astro-comb peak visible on HARPS-N with a previously derived HARPS-N line profile and use residuals from a fit of line

centers to a sixth order polynomial. We find systematic residual offsets of approximately 3 millipixels every 256 pixels in the dispersion direction of the CCD. Note that as expected by the CCD manufacturer, these offsets are significantly smaller than observed using a similar technique at the original HARPS spectrograph[11].
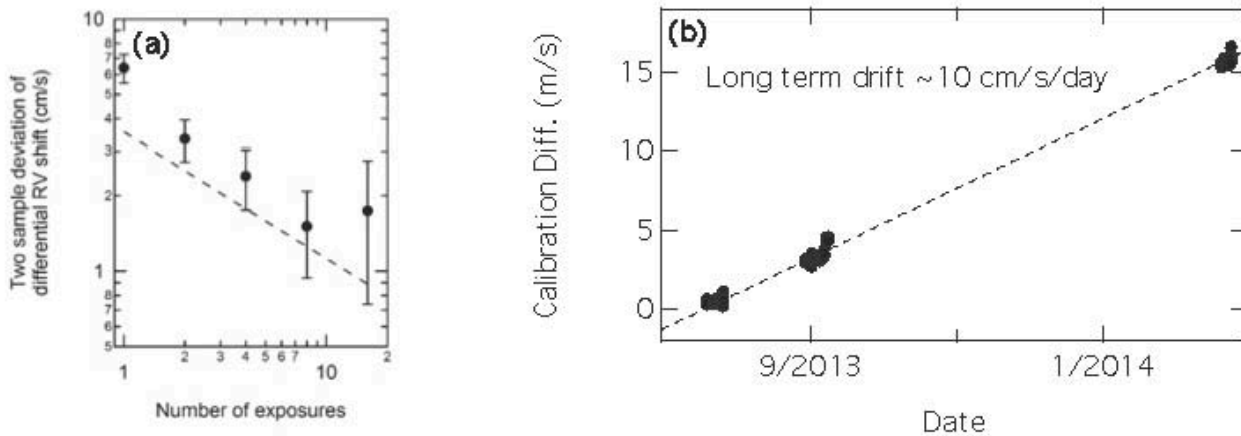


Figure 11 - Short-term sensitivity of astro-comb in measuring HARPS-N spectrograph as represented by the two sample deviation of the difference between the calibrations of the two HARPS-N fibers when both are illuminated by astro-comb light, with one sigma error bars. Differences between exposures are derived from cross-correlations with the sum of all exposures. Dashed line is the expected photon shot noise limit. (b) Long-term stability of HARPS-N spectrograph when using simultaneous calibration. Shown is the difference in calibration between the science and calibration fibers as measured with the astro-comb.

## 6.2 Future improvements: Automation of laser-comb alignment

The astro-comb has been operating at the TNG/HARPS-N since January of 2013. Currently, a laser expert is required to operate the system. Thus the astro-comb has been operated for roughly 11 out of the past 70 weeks. To improve the uptime of the astro-comb, we are currently implementing automation of the system. Recent upgrades at the TNG include auto-alignment of the flat mirror Fabry-Perot filter cavities and of the PCF wavelength shifting fiber. Between exposures, we scan the input coupling of the PCF and measure the output spectrum on a low resolution optical spectrum analyzer to automatically optimize the astro-comb spectral bandwidth. This leads to push-button reproducibility of spectral coverage with the astro-comb. Similarly, the alignment of the Fabry-Perot filter cavities are automatically aligned to optimize the finesse of the cavities.

Work on automatic start-up and fine alignment of the titanium:sapphire laser continues in the laboratory to be implemented at the TNG in the coming year.

# 7.   RECENT HARPS-N SCIENCE HIGHLIGHTS

## 7.1  The GAPS Programme with HARPS-N at TNG. III: The retrograde orbit of HAT-P-18b

(Esposito, M. et al., 2014, A&A, 564, 13)

The very precise radial velocity measurements delivered by the HARPS-N were used to measure the Rossiter-McLaughlin effect for Saturn-mass planet HAT-P-18b, which orbits one of the coolest stars for which the effect has been measured so far. HAT-P-18b was found to lie on a counter-rotating orbit, the sky-projected angle between the stellar spin axis and the planet orbital axis being $\lambda = 132 \pm 15$ deg. This planet is one of the few known so far to transit a star with Teff $\lesssim 6250$K on a retrograde orbit, and the objects as this most likely have a weak tidal coupling with their parent stars, therefore their orbits preserve any original misalignment. As such, they are ideal targets to study the causes of orbital evolution in cool main-sequence stars.

## 7.2  An Earth-sized planet with an Earth-like density

(Pepe, F. et al., 2013, Nature, 503,377)

Recent analyses of data from the NASA Kepler spacecraft have established that planets with radii within 25 per cent of the Earth's are commonplace throughout the Galaxy, orbiting at least 16.5% Sun-like stars. These studies were sensitive to the sizes of the planets but not their masses, so the question remains whether these Earth-sized planets are indeed similar to the Earth in bulk composition. In this work the authors used HARPS-N to observe an Earth-sized planet Kepler-78b, which was found by Kepler to have a radius of only 1.16 times that of the Earth. Thanks to the precise radial velocity measurements provided by HARPS-N, the authors estimated that the mass of this planet is 1.86 Earth masses. The resulting mean density of the planet is 5.57 g/cm$-3$, which is similar to that of the Earth and implies a composition of iron and rock.

## 7.3  The GAPS programme with HARPS-N at TNG. II. No giant planets around the metal-poor star HIP 11952

(Desidera, S. et al., 2013, A&A, 554, 29)

The authors of the study have performed radial velocity monitoring of the metal-poor star HIP 11952 on 35 nights during about 150 days using HARPS-N at the TNG. HIP 11952 was believed to host a planetary system of two giant planets with periods of $6.95 \pm 0.01$ and $290.0 \pm 16.2$ days, as a previous recent study announced. The results of the analysis of the radial velocities from HARPS-N excluded the presence of the two giant planets. This result is important because HIP 11952 was thought to be the most metal-poor star hosting a planetary system with giant planets, thus challenging some models of planet formation.

## 7.4  The GAPS programme with HARPS-N at TNG. I. Observations of the Rossiter-McLaughlin effect and characterization of the transiting system Qatar-1

(Covino, E. et al., 2013, A&A, 554, 28)

In this paper the HARPS-N high-precision radial velocity measurements were exploited to measure the Rossiter-McLaughlin effect in the Qatar-1 system. The orbital solution for the Qatar-1 system was found to be consistent with a circular orbit and a sky-projected obliquity of $\lambda = -8.4 \pm 7.1$ deg. The results of the work show that the system is well aligned and fits well within the general $\lambda$ versus Teff trend. The planet, with a mass of $1.33 \pm 0.05$ Jupiter masses, is found to be significantly more massive than previously reported, while the host star is confirmed to be metal-rich and slowly rotating, though moderately active, as indicated by the strong chromospheric emission in the Ca II H&K line cores.

### 7.5 KOI-200 b and KOI-889 b: Two transiting exoplanets detected and characterized with Kepler, SOPHIE, and HARPS-N

(Hébrard, G. et al., 2013, A&A, 554, 114)

In this work, partially based on HARPS-N data, the detection and characterization of the two new transiting, close-in, giant extrasolar planets KOI-200 b and KOI-889 b is reported. First identified by the Kepler team as promising candidates from photometry of the Kepler satellite, the targets were then observed with spectrographs SOPHIE and HARPS-N and thanks to the precise radial velocity data, their planetary nature was established. Combined analyses of the whole datasets show that the planet KOI-200 b has mass and radius of $0.68 \pm 0.09$ MJup and $1.32 \pm 0.14$ RJup, while the planet KOI-889 b is a massive planet with mass and radius of $9.9 \pm 0.5$ MJup and $1.03 \pm 0.06$ RJup. These two planets are among the first detected and characterized thanks to observations secured with HARPS-N, then recently mounted at the TNG.

## REFERENCES

[1] Cosentino Rosario, et al., "Harps-N: the new planet hunter at TNG",
Ground-based and Airborne Instrumentation for Astronomy IV. Proceedings of the SPIE, Volume 8446, article id. 84461V, 20 pp. (2012)

[2] Esposito M. et al., "The GAPS Programme with HARPS-N at TNG. III: The retrograde orbit of HAT-P-18b" , Astronomy & Astrophysics, Volume 564 (2014)

[3] Pepe F. et al.," An Earth-sized planet with an Earth-like density", Nature, Volume 503, Issue 7476, pp. 377-380 (2013)

[4] Desidera S. et al., "The GAPS programme with HARPS-N at TNG. II. No giant planets around the metal-poor star HIP 11952 ", Astronomy & Astrophysics, Volume 554 (2013)

[5] Covino E. et al., "The GAPS programme with HARPS-N at TNG. I. Observations of the Rossiter-McLaughlin effect and characterisation of the transiting system Qatar-1", Astronomy & Astrophysics, Volume 554 (2013)

[6] Hébrard G. et al., "KOI-200 b and KOI-889 b: Two transiting exoplanets detected and characterized with Kepler, SOPHIE, and HARPS-N ",Astronomy & Astrophysics, Volume 554 (2013)

[7] Li  C.-H., et al. , " Green astro-comb for HARPS-N" Proc. SPIE 8446, Ground-based and Airborne Instrumentation for Astronomy IV, 84468X (2012)

[8] Ycas G. G., et al. , "Demonstration of on-sky calibration of astronomical spectra using a 25 GHz near-ir laser frequency comb," Opt. Express 20 , 6631-6643 (2012).

[9] Wilken  T., et al. , "A spectrograph for exoplanet observations calibrated at the centimetre-per-second level," Nature 485 , 611-614 (2012).

[10] Phillips D. F., et al. , "Calibration of an astrophysical spectrograph below 1 m/s using a laser frequency comb" Opt. Express 20 , 13711-13726 (2012)

[11] Wilken  et al. , "High-precision calibration of spectrographs," Mon. Not. R. Astron. Soc. Lett. 405, L16-L20 (2010).

[12] Molinari  E., Hernendez, N., 2014, Montreal SPIE Conference 9149-82

[13] Barbieri  C., Optical Telescopes of Today and Tomorrow, Proc. SPIE Vol. 2871, p. 244-255(1997)

[14] Mayor M., Pepe F. Queloz D. et al., The Messenger (ISSN0722-6691), No.114, p. 20-24 (December 2003)

[15] Sosnowska D. Vick A., Lodi M., et al., Astronomical Telescopes + Instrumentation, SPIE Conference Proceeding, 8451-68 (2012)

[16] Wildi F., Chazelas B., Pepe F., "A passive cost-effective solution for the high accuracy wavelength calibration of radial velocity spectrographs", Ground-based and Airborne Instrumentation for Astronomy IV. Proceedings of the SPIE, Volume 8446

[17] Wildi F., et al., "The performance of the new Fabry-Perot calibration system of the radial velocity spectrograph HARPS", Techniques and Instrumentation for Detection of Exoplanets V. Edited by Shaklan, Stuart. Proceedings of the SPIE, Volume 8151, article id. 81511F

[18] Fischer Debra A., et al., "A Sub-Saturn Mass Planet Orbiting HD 3651",The Astrophysical Journal, Volume 590, Issue 2, pp. 1081-1087